Influence of the Borate on the Performance of ASA-Al_2O_3 supported Ni-Mo Hydrocracking Catalyst

Taghizadeh Yusefabad, Ehsan; Tavasoli, Ahmad*[+]

School of Chemistry, College of Science, University of Tehran, Tehran, I.R. IRAN

Zamani, Yahya

Gas Division, Research Institute of Petroleum Industry, Tehran, I.R. IRAN

ABSTRACT: *The borate-doped and non-borated Ni-Mo/ASA-Al_2O_3 catalysts have been prepared and characterized by the BET, XRD, TGA, and NH_3-TPD analysis. The catalyst's performance was assessed in n-hexadecane hydrocracking using a downflow fixed bed micro-reactor. The stability of the catalysts in the presence of water and coke deposition was examined for the HCK of non-conventional feeds. The obtained results revealed that borate increased the feed percentage conversion from 91.43 to 99.21% compared to the not borated catalyst. This improvement is mostly due to the promotion of the acidic functions by BO_3 addition. Results showed that the addition of borate increased the selectivity of light hydrocarbons and light gaseous products slightly (from 4.64 to 8.76%).*

KEYWORDS: *Hydrocracking (HCK); Ni-Mo Catalyst; Borate; Discrete lumping model; VGO.*

INTRODUCTION

Since petroleum sources are changing into heavy and extra-heavy crude oils, the quality of crude oil is decreasing [1,2]. These heavy crudes have a high amount of residual bottom and their fractionation renders low amounts of distillates with a large investment in distillation plants. Hence, it is necessary to upgrade heavy crudes before distillation [3] and convert the large molecules (mainly asphaltenes) into low molecular weight fractions, preferably middle distillates and gasoline, while removing the sulfur, nitrogen, and metal impurities [3]. Hydrocracking is employed to convert heavy oil fractions into valuable products [4-7]. The development of high-active and selective hydrocracking catalysts is important in studies about this process. The hydrocracking catalysts are bifunctional systems: sulfided Ni-Mo-S component often performs hydrogenating properties and acidic component performs cracking properties. Zeolites, Aluminosilicates can be used as an acidic components [8]. Catalysts based on the Aluminosilicates are less active but more selective to middle distillates [8,10], and the zeolite-containing catalysts are rapidly deactivated by heteroatomic compounds [11-15]. The preparation of catalysts with enhanced properties could be achieved in three ways: new support, active species and promoters [15]. The boron increases the acidic nature of metal oxides catalysts. This increased acidity makes

* *To whom correspondence should be addressed.*
+ *E-mail: tavasoli.a@ut.ac.ir*
1021-9986/2021/4/1247-1255 9/$/5.09

enhance the cracking and isomerization activity of the catalysts [[15,16,32]]. Many investigations studied the effect of boron on Al_2O_3 with Co-Mo and Ni-Mo as the active species [17- 20]. In 1999, the Author links and *Yu-WenChenMing-ChangTsai* [21] investigated hydrotreating of residue oil over a series of aluminum borate-supported CoMo and NiMo catalysts. They concluded that these catalysts were more active than the alumina-supported catalysts [21]. In 2000, *M Lewandowski* and *Z Sarbak* [22] Studied catalytic activity of a series of nickel–molybdenum catalysts supported on Al_2O_3 modified with borate ions for the hydrotreating of coal liquid. It was found that modification of the support with borate ions increases the acidity of nickel–molybdenum catalyst, in particular, the number of acidity centers of intermediate strength[22]. In 2004, D. Ferdous et al. [23] investigated a series of $NiMo/Al_2O_3$ catalysts containing boron and phosphorus. It was found that the addition of boron to $NiMo/Al_2O_3$ caused an increase in weak acid centers, whereas phosphorus caused the formation of acid centers with intermediate strength [23]. In 2006, *D. Ferdous et al.* [24] comprised product selectivity during hydroprocessing of bitumen-derived gas oil in the presence of $NiMo/Al_2O_3$ catalyst containing boron and phosphorus. It was found that phosphorus-containing catalysts showed excellent hydrocracking and mild hydrocracking activities at all operating conditions [24]. In 2012, *Radostina Palcheva et al*. [25] investigated $NiMo/\gamma\text{-}Al_2O_3$ Catalysts. they found that the addition of Co, Ni, or B influenced the Al_2O_3 phase composition and gave increased catalytic activity for 1-benzothiophene hydrodesulfurization (HDS). They proved that the prior loading of Ni, Co, or B increased the degree of sulfidation of the $NiMo/\gamma\text{-}Al_2O_3$ catalysts[25]. In 2013, *WenbinChen et al*. [26] investigated the effect of modification of the alumina acidity on the properties of supported Mo and CoMo sulfide catalysts. In this investigation, aluminas with different boron loadings were prepared by impregnation with H_3BO_3 solutions and then used to prepare pure Mo and CoMo catalysts. The results point out a relationship between the Brønsted acidity of the support and the electronic properties of the MoS_2 and CoMoS phase [26]. *P.P. Dick et al.* reported on the excellent characteristics of Ni-Mo catalysts supported on $ASA\text{-}Al_2O_3$ [19] on the VGO hydrocracking. In this research, we look at the effect of the boron functional group on $Ni\text{-}Mo/ASA\text{-}Al_2O_3$ catalyst at 0.0 wt%, 1.8 wt% and 3.6 wt% loadings. The aim of the present work is to investigate if the addition of boron to the $Ni\text{-}Mo/ASA\text{-}Al_2O_3$ catalyst will lead to further enhancement of activity and selectivity and finding the optimum amount of the boron. The catalysts were characterised by a number of techniques such as X-Ray Diffraction (XRD), Brunauer–Emmett–Teller (BET), and NH_3 temperature-programmed desorption (NH_3-TPD), and also quantitative analysis of the coke formed has been carried out by means of thermogravimetric-analysis (TGA). Performance of the mentioned catalysts was investigated in the n-hexadecane (n-C16) hydrocracking and liquid products were analyzed by Gas Chromatography-Mass Spectroscopy (GCMS).

EXPERIMENTAL SECTION

Materials

The commercial Alumina, Ammonium heptamolybdate, and Nickle nitrate were provided from Tehran Oil Refinery (Iran). N-Hexadecane, as feedstock, was purchased from (Merck, Darmstadt Germany).

Methods

Preparation of the $ASA\text{-}Al_2O_3$, $ASA\text{-}Al_2O_3\text{-}B_{1.8}$, and $ASA\text{-}Al_2O_3\text{-}B_{3.6}$ supports

$ASA\text{-}Al_2O_3$ support was prepared according to the following method. The support contains 70% of $Al_2O_3\text{-}SiO_2$ and 30% $\gamma\text{-}Al_2O_3$. $Al_2O_3\text{-}SiO_2$ is containing $\gamma\text{-}Al_2O_3$ and 90wt.% SiO_2. The mixture of powders was loaded into the mixer with Z-folded blades. Then the mixture was peptized by nitric acid under stirring for 30 min (acid modulus 0.03–0.05). The obtained paste was extruded using plunger extruder VINCI with a Teflon spinneret with trilobular hole at a pressure of 3.5–4.0 MPa and a velocity of plunger moving of 1.2 mm/s. Extrudates were dried for 4 h at 120◦C in airflow and then heated for 2 h to 415◦C and calcined at 415◦C for 4 h. Then 30% of $\gamma\text{-}Al_2O_3$ was added to the above mixture. Extrudates were dried and calcined as above.

The obtained powder is divided into three parts and aqueous solutions of 1.8 and 3.6wt.% HBO_3 are prepared and added to two parts of the obtained support, separately. Extrudates were dried and calcined. Circumscribe circle

diameters of extrudates were not more than 1.5 mm in this case. The obtained supports are hereafter denoted as ASA-Al_2O_3-B_0, ASA-Al_2O_3-$B_{1.8}$, and ASA-Al_2O_3-$B_{3.6}$.

Preparation of the catalyst

Nickel–molybdenum supported catalysts were prepared by the incipient wetness co-impregnation method (pH ≈ 5.4) using aqueous solutions with the appropriate amounts of nickel nitrate and ammonium heptamolybdate to obtain 15.0 wt.% MoO_3 and 4.0 wt.% NiO respectively. The impregnated catalysts were dried in air at 120 ◦C and calcined at 415 ◦C for 4 h. The supported catalysts are hereafter denoted as NiMo/ASA-Al_2O_3-B_0, NiMo/ASA-Al_2O_3-$B_{1.8}$, and NiMo/ASA-Al_2O_3-$B_{3.6}$, respectively.

Catalyst characterization

The BET surface area (S_{BET}), Pore Size (PS) distribution, and pore volume (PV) of the catalysts were measured by conducting nitrogen adsorption/desorption analysis using Micromeritics ASAP 2010 at 77 K. Prior to analysis, the sample was degassed at 350 ºC for 8 h. Barret–Joyner–Hallender (BJH) model on desorption branch was employed to calculate the pore size distributions. The micropore surface area of the catalysts was obtained from the corresponding t-plot.

XRD patterns of the catalysts were recorded using a Bruker Advance diffractometer with Da Vinci geometry using Ni-filtered CuK _α radiation (40 kV, 30 mA) instrument. Catalysts (0.2 g) were ground in a mortar to a particle size of 38 μm. The occurrence of the respective oxidized species of the metals incorporated wide-angle analyses was performed for all catalysts. In this case, 2θº range was scanned between 10º and 80º. By comparing the observed pattern with the diffraction pattern reported in the database PDF-4 + ICDD (SiO_2-00-058-0344) qualitative analysis of the observed peaks was carried out.

NH_3 Temperature - Orogrammed Desorption (NH_3-TPD) was performed to determine the relative acidity of the samples at ICB-CSIC in a Micromeritics Pulse Chemisorb 2700. A sample consisting of 200 mg was outgassed in Ar flow to desorb water and impurities from the sample. To do this, the sample was heated at a rate of 10 °C/min from room temperature to 600 °C and held at this temperature for 60 min. The sample was then cooled down to 50 °C and ammonia was introduced into the system; the physically adsorbed ammonia was purged afterward. The system was heated at a rate of 10 °C/min to 600 °C and the chemisorbed ammonia was determined with a thermoconductivity detector (TCD). The TCD read the NH_3 concentration, which was converted into μmol/g.min unit and then plotted against the temperature. The number of acid sites was determined by integrating the area under the curve for each type of acidity (weak, medium, and strong) and expressed in molecules of NH_3 adsorbed per temperature interval.

The carbonaceous deposited on the spent catalysts was determined using a Pyris TGA1 thermogravimetric analyzer. First, 3 mg samples were heated from 100 to 700 ˚C with a heating rate of 10˚C/min under airflow of 40 mL/min. Then the samples were held at isothermal conditions for the initial and final temperatures to allow the stabilization of the weight of the catalyst. The coke deposits were determined as a difference between weight loss of the fresh and spent carbon-supported catalysts in the region where coke deposits were occurred (200–500^{O}C).

Testing of the catalysts in hydrocracking of n-hexadecane

N-hexadecane hydrocracking was carried out on a steel tubular fixed-bed up-flow reactor. The experimental setup was depicted in Fig. 1. About the 1.00 gr catalyst was filled in the reactor and reduced by H_2 gas at pressure 30 bar and a space velocity of 200 h^{-1} with constant heating rate from ambient to 453 K and maintained at this temperature for 1 h. To prepare Ni-Mo-S phases, the catalysts were sulfided by a stream of 1wt% of dimethyl disulfide in hexane. Conditions of the sulfidation are as follows: hydrogen atmosphere with an H_2/Oil volumetric ratio of 80 nl/L at a space velocity of 200 h^{-1} and 30 bar. The samples were heated with a constant heating rate of 0.5 K/min from 453 to 633 K and kept at the temperature, 633K, for 10 h. The performances of catalysts were evaluated in n-C16 hydrocarbons process. Conditions of the reaction are as follows: Injection rate of 30 cm^3/h and H_2/Oil = 175 nL/L, 30 bar, WHSV = 3 kg/ (L·h), LHSV = 4.2 h^{-1}. The reaction temperature was 573 K. After catalyst testing, the reactor was depressurized under hydrogen flow at 573 K for 3 h. Then, the flow was switched to nitrogen and the temperature decreased to room temperature. Liquid products produced during the reaction were analyzed. The used experimental setup was depicted in Fig.1.

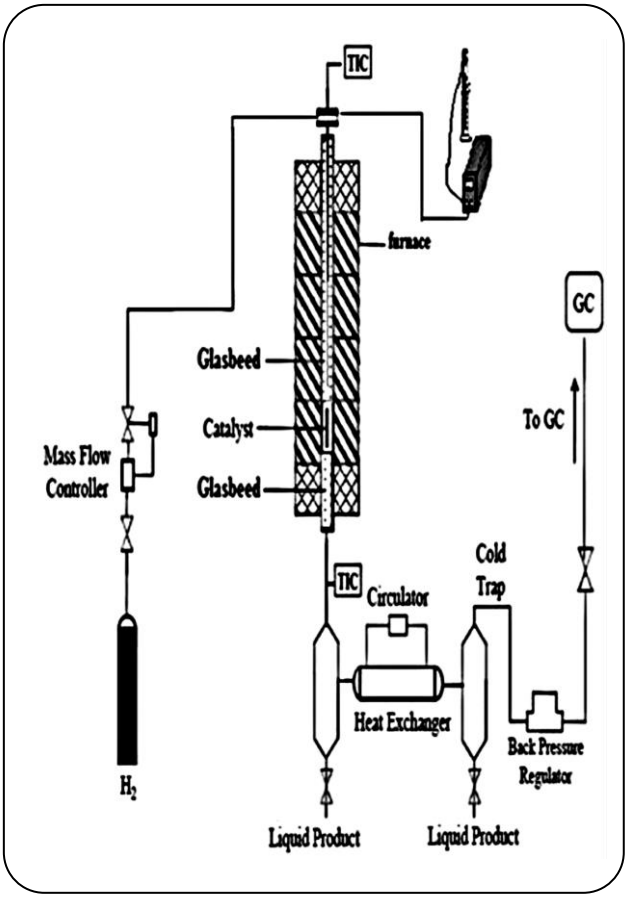

Fig. 1: Schematic of the experimental setup.

GCMS of liquid products

Liquid products were recovered after each reaction and were analyzed by gas chromatography (GC). An Agilent Technologies 7890A Chromatographer fitted with a Mass Selective detector (5975C VL MSD with Triple-Axis Detector) was used to measure the amount of each fraction distribution below 230ºC in the liquid product. The GC was equipped with a capillary column (Rtx 5 MS, HT-30 m long, 25μm film thickness) and was operated in split mode (split ratio 1:25) with helium as a carrier gas. A calibration using Data processed by Agilent MSD Chemistation (Rev E.02.02.1413) was performed to evaluate the percentage of the material. The temperature program of GC-mass is listed in Table 3.

RESULTS AND DISCUSSION

Catalysts characterization

The XRD patterns of the NiMo/ASA-Al_2O_3-B_0, NiMo/ASA-Al_2O_3-$B_{1.8}$, and NiMo/ASA-Al_2O_3-$B_{3.6}$ catalyst are illustrated in Fig. 3. The γ-alumina, SiO_2, NiO, MoO_3 phases are observed in the XRD patterns of these catalysts, however, $AlBO_3$ phases are observed in the XRD pattern of the NiMo/ASA-Al_2O_3-$B_{1.8}$, and NiMo/ASA-Al_2O_3-$B_{3.6}$ catalysts. Three diffraction peaks that are appeared at the 2θ values of 25.7, 61.6, and 66.6 are assigned to γ-Al_2O_3 [27][27]. However, the observed peaks for the Ni-Mo/ASA-Al_2O_3-B_0 catalyst were broader than that of the NiMo/ASA-Al_2O_3-$B_{1.8}$, and NiMo/ASA-Al_2O_3-$B_{3.6}$ catalysts. Three main diffraction peaks for SiO_2 are located at 2θ values of 20.7, 23.5, and 66.6. The main diffraction peak that is appeared at 2θ values of 36.9 is assigned to NiO. Three main diffraction peaks for MoO_3 are located at 2θ values of 23.5, 25.7, and 27.4. The observed peaks revealed that the MoO_3 particles were well dispersed on the catalyst's surface. Three diffraction peaks that are appeared at 2θ values of 39.6, 48.9, and 58.6 are assigned to $AlBO_3$. By comparing the mentioned patterns, it can be seen that the peaks of the NiMo/ASA-Al_2O_3-B_0 catalysts are at a lower energy level than those of the NiMo/ASA-Al_2O_3-$B_{1.8}$, and NiMo/ASA-Al_2O_3-$B_{3.6}$ ones.

Textural properties of the mentioned catalysts are reported in Table 4.

According to table 4, the addition of borate to the catalyst decreased the BET surface area and pore volume. However, due to the blockage of small pores, the average pore sizes increased by adding the borate.

N_2 Adsorption–desorption isotherms and corresponding BJH pore size distributions for the NiMo/ASA-Al_2O_3-B_0, NiMo/ASA-Al_2O_3-$B_{1.8}$, and NiMo/ASA-Al_2O_3-$B_{3.6}$ catalysts are shown in Fig. 4.

The shape of N_2 adsorption-desorption isotherm for Ni-Mo/ASA-Al_2O_3 is type IV, which displays mesoporous materials. The hysteresis loop for this catalyst can be categorized into H_2 type [27]. On the other hand, the hysteresis loop for the catalyst prepared in the presence of HBO_3 exhibits a mixture of cylinder type (H1) of pores [27]. As shown, textural properties are affected by the incorporation of HBO_3. The addition of HBO_3 leads to a decrease in low diameter mesoporous.

Results for acidity studies performed using ammonia Temperature-Programmed Desorption (NH_3-TPD) are presented in Table 5.

Table 3: Temperature program of GC-mass.

Parameter	Step 1
Initial Temperature (ºC)	60
Initial Time (min)	1
Program Rate (ºC/min)	10
Final Temperature (ºC)	250
Final Time (min)	40
Split ratio (ml/min)	25
Septum purge (ml/min)	6
Flow rate (ml/min)	1

Table 4: Textural Properties of NiMo Catalysts.

Catalyst	S_{BET}[a] (m^2/g)	V_{total}[b] (Cm^3/g)	d_{avr}[c](Å)
NiMo/ASA-Al_2O_3-B_0	158.19	0.39	99.24
NiMo/ASA-Al_2O_3-$B_{1.8}$	144.17	0.38	105.27
NiMo/ASA-Al_2O_3-$B_{3.6}$	142.49	0.38	105.49

[a] *Specific surface area* [b] *Pore volume* [c] *Average pore size*

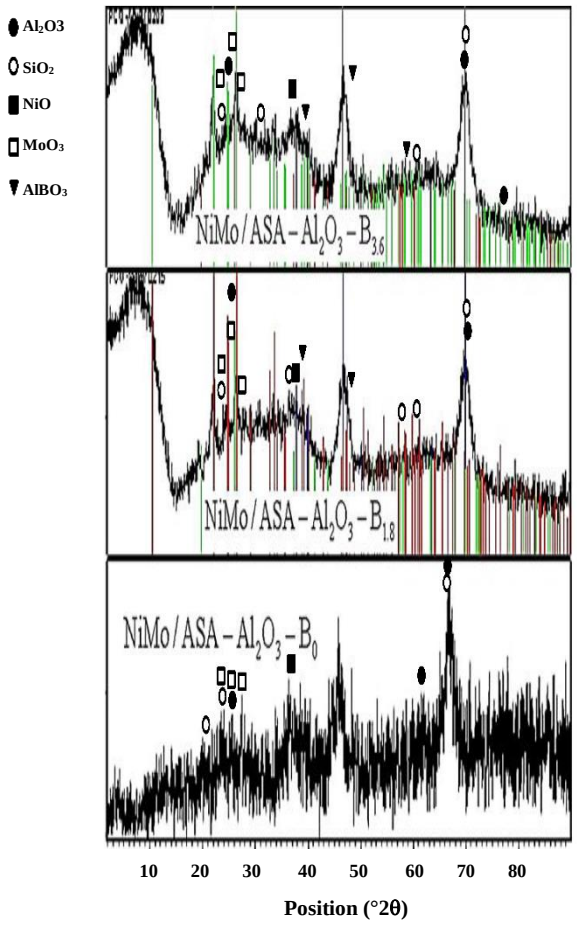

Fig. 2: Powder XRD patterns of the NiMo/ASA-Al_2O_3-B_0, NiMo/ASA-Al_2O_3-$B_{1.8}$, and NiMo/ASA-Al_2O_3-$B_{3.6}$ catalyst.

The NH_3-TPD profiles are decomposed by fitting, and the acidity densities of two major acid sites I and II estimated by the integrated areas are listed in Table 5. The loadings of borate into the Ni-Mo/ASA-Al_2O_3-B_0 catalyst significantly change the structure of surface acid sites. Table 5 shows a low-temperature peak at about 260°C (the site I) and a high-temperature peak at about 410°C (site II). The high-temperature site is related to protonic acidity, while the low-temperature site is probably due to ammonia coordinated to aluminum species. In this study, the reaction was carried out at a temperature 300° C, so acid site I should be considered for the analysis of acidic properties on the process. It was observed that the NiMo/ASA-Al_2O_3-$B_{1.8}$, and NiMo/ASA-Al_2O_3-$B_{3.6}$ catalysts had higher acidities than the Ni-Mo/ASA-Al_2O_3-B_0 catalyst across several temperature ranges. Since the cracking function of the Ni-Mo/ASA-Al_2O_3-B_0 catalyst was low, borate loading was chosen for the catalyst. The Ni-Mo/ASA-Al_2O_3-B_0 catalyst presented lower acidity, which could result in reducing the cracking activity. It would be expected that the more acidic catalysts would have a stronger cracking function [28,29].

TCD signals of these three catalysts are shown in Fig. 3.

In addition to the catalyst acidity, inactivation by a coke can be an important factor in catalytic properties of the catalysts. So, the impact of process conditions and feedstock conversions on the coke formation should be considered [5]. The results of TGA analysis of the catalysts have been illustrated in Table 7.

Table 5: Acid Amount of the Catalysts.

Catalyst	Acid amount [mmol/g-cat]			
	Acid site I		Acid site II	
	Strength (° C)	Density (mmol/g)	Strength (° C)	Density (mmol/g)
NiMo/ASA-Al_2O_3-B_0	263	0.8863	420	0.6574
NiMo/ASA-Al_2O_3-$B_{1.8}$	261	0.9352	411	0.5288
NiMo/ASA-Al_2O_3-$B_{3.6}$	262	0.9836	405	0.3376

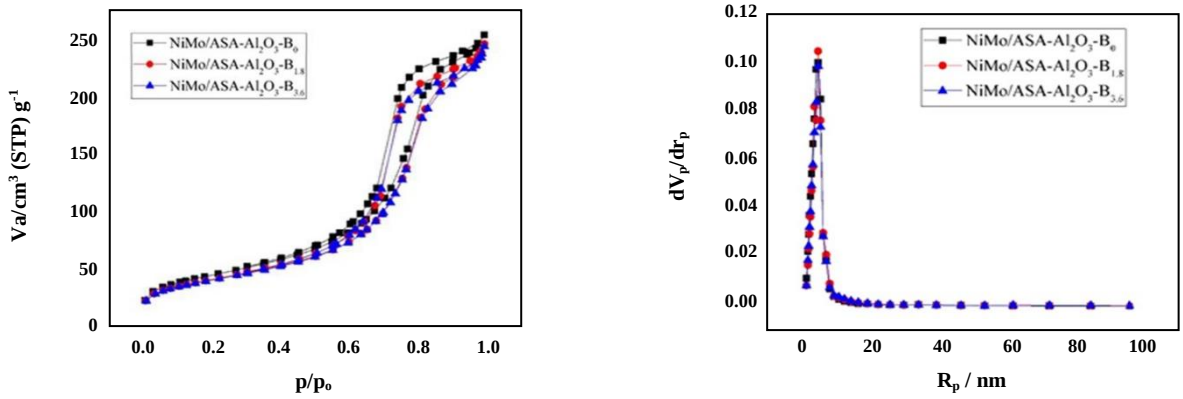

Table 4: N_2 adsorption-desorption isotherms and corresponding BJH pore size distributions for the NiMo/ASA-Al_2O_3-B_0, NiMo/ASA-Al_2O_3-$B_{1.8}$, and NiMo/ASA-Al_2O_3-$B_{3.6}$ catalysts

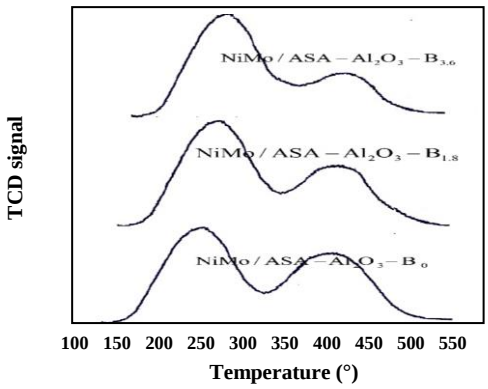

Fig. 3: The TCD signal with respect to the temperature for the NiMo/ASA-Al_2O_3-B_0, NiMo/ASA-Al_2O_3-$B_{1.8}$, and NiMo/ASA-Al_2O_3-$B_{3.6}$ catalysts

One of the important benefits of using the dispersed catalyst for the conversion of heavy feedstocks is the inhibition of coke formation [29]. The coke formation on the catalyst and deactivation of that could be affected by catalyst activity [15]. Coke produced by the polymerization of n-C16 and products will cover the active sites in hydroprocessing reactions [15]. The rate of isomerization in the presence of the borated catalyst could be more than that of the un-borated one. Although the amount of the produced coke increased on the catalyst, due to the increase in catalyst acidity, the rate of increase in conversion can be justified.

N-hexadecane hydrocracking

To study the effect of the catalyst formulation on n-C16 hydrocracking, the NiMo/ASA-Al_2O_3-B_0, NiMo/ASA-Al_2O_3-$B_{1.8}$, and NiMo/ASA-Al_2O_3-$B_{3.6}$ catalysts were prepared with identical porosity, identical active phase, and variation in the acid strength. Their performances were then evaluated in the reactor. Before the reaction test, the catalyst was sulfided by a stream of 1wt% of dimethyl disulfide in n-hexane under the hydrogen atmosphere. The activity of the catalysts for the n-hexadecane hydrocracking has been investigated at a temperature of 573 K with an H_2/hydrocarbon molar ratio of 175 at a total pressure of 3 MPa. The total percentage of the products achieved during n-C16 hydrocracking in the presence of the NiMo/ASA-Al_2O_3-B_0, NiMo/ASA-Al_2O_3-$B_{1.8}$, and NiMo/ASA-Al_2O_3-$B_{3.6}$ catalysts are given in table 6.

Table 7: Coke deposition results of the NiMo/ASA-Al_2O_3-B_0, NiMo/ASA-Al_2O_3-$B_{1.8}$, and NiMo/ASA-Al_2O_3-$B_{3.6}$ catalysts.

catalyst	Coke (wt. %)
NiMo/ ASA-Al_2O_3-B_0 spent	18.95
NiMo/ASA-Al_2O_3-$B_{1.8}$ spent	19.53
NiMo/ASA-Al_2O_3-$B_{3.6}$ spent	19.92

Table 6: Total percentage of the products achieved in presence of different catalysts

Catalyst	Conversion(%)	Gasous products(%)	Liquidic products(%)
NiMo/ ASA-Al_2O_3-B_0	91.43	4.64	95.36
NiMo/ASA-Al_2O_3-$B_{1.8}$	96.38	7.65	92.35
NiMo/ASA-Al_2O_3-$B_{3.6}$	99.21	8.76	91.24

As shown in Table 6, the n-C16 was until about 91.43 percent cracked into smaller hydrocarbons in the presence of the Ni-Mo/ ASA-Al_2O_3-B_0 catalyst, 96.38 percent in the presence of the Ni-Mo/ASA-Al_2O_3-$B_{1.8}$ catalysts, and 99.21 percent in the presence of the Ni-Mo/ASA-Al_2O_3-$B_{3.6}$ catalysts. In other words, the presence of the borate-functional group enhances the hydrocracking activity. Table 6 show that by increasing the borate functional group to the Ni-Mo/ASA-Al_2O_3-B_0 catalyst, the amount of the liquid products decreases, and the amount of gas products increases. The increase in the conversion with increasing the borate functional to the catalyst could be due to increasing the acidity of the catalysts. This is in accordance with reference [15]. The molar distribution of the liquid products is shown in Fig. 6.

According to Fig. 5, the selectivity of the liquid products from the n-C16 hydrocracking in the presence of the Ni-Mo/ASA-Al_2O_3-B_0 catalyst is the C10 compounds, C9 compounds in presence of NiMo/ASA-Al_2O_3-$B_{1.8}$, and the C8 compounds in the presence of Ni-Mo/ASA-Al_2O_3-$B_{3.6}$. the conversion and selectivity in the HCK process can be impacted by several factors such as the zeolite porosity, the hydrogenation on the acidity ratio (site strengths and numbers), or the proximity between the two catalytic functions [6]. The data in table 6 and figure 5 show the cracking properties of the hydrocracking catalysts strongly depend on their acidic characteristics [6,28,29].

Hydrocracking takes place on the Brønsted acid sites [30,31]. Accordingly, the activity of supports follows the same trend as Brønsted acidity with the support composition. In a bi-functional catalyst, the balance between the two catalytic functions highly impact the catalytic properties [31]. Improved strength of the hydrogenation

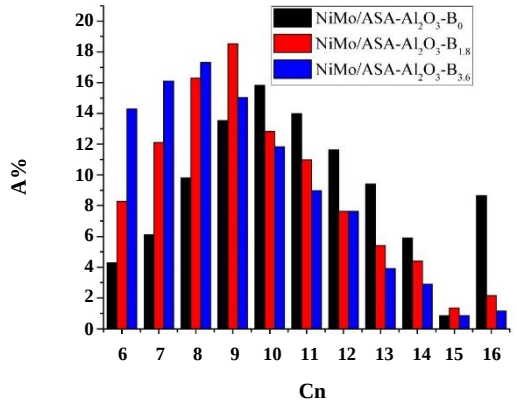

Fig. 6: Molar distribution of the products in the conversion of n-hexadecane in the presence of the NiMo/ASA-Al_2O_3-B_0, NiMo/ASA-Al_2O_3-$B_{1.8}$, and NiMo/ASA-Al_2O_3-$B_{3.6}$ catalysts

the function can result in a significant increase in the conversion and selectivity towards desired products by increasing the rate of the carbocation desorption, reducing the rate of acid site deactivation, and limiting the extent of secondary cracking. Therefore, the ratio between the two catalytic functions of the prepared catalysts is not affected by a modification of the hydrogenation properties [6].

CONCLUSIONS

In this study, the NiMo/ASA-Al_2O_3-B_0, NiMo/ASA-Al_2O_3-$B_{1.8}$, and NiMo/ASA-Al_2O_3-$B_{3.6}$ catalysts were synthesized by incipient wetness impregnation. The n-hexadecane hydrocracking process were carried out in an experiment-scale fixed-bed reactor. The synthesized catalysts were characterized using X-Rray Diffraction (XRD), Brunauer–Emmett–Teller (BET), and NH_3-Temperature Programmed Desorption (NH_3-TPD), and also quantitative

analysis of the coke formed has been carried out by means of ThermoGravimetric-Analysis (TGA). The effect of adding borate to the NiMo/ASA-Al_2O_3 catalyst was investigated. It was observed that:

1- The addition of borate to the catalyst decreased the BET surface area and pore volume. However, due to the blockage of small pores, the average pore sizes increased with adding the borate.

2- The activity of the catalyst (Ni-Mo/ASA-Al_2O_3) goes up with adding boric acid.

3- Boric acid could increase the catalyst acidity.

Received : Nov. 22, 2019 ; Accepted : Feb. 17, 2020

REFERENCES

[1] LI W., ZHU J., and QI J., Application of Nano-Nickel Catalyst in the Viscosity Reduction of Liaohe Extra-Heavy Oil by Aqua-Thermolysis, *J. Fuel Chem. Technol.*, **35(2)**: 176–180 (2007).

[2] Martínez-Palou R., de LourdesMosqueira M., Zapata-Rendón B., Mar-Juárez E., Bernal-Huicochea C., de la Cruz Clavel-López J., Aburto J., Transportation of Heavy and Extra-Heavy Crude Oil by Pipeline: A Review, *J. Pet. Sci. Eng.*, **75(3)**: 274–282 (2011).

[3] Leyva C., Ancheyta J., Travert A., Maugé F., Mariey L., Ramírez J., S.Rana M., Activity and Surface Properties of NiMo/SiO_2–Al_2O_3 Catalysts for Hydroprocessing of Heavy Oils, *Appl. Catal. A Gen.*, 425–426, 1–12 (2012).

[4] Utami M., Wijaya K., Trisunaryanti W., Pt-Promoted Sulfated Zirconia as Catalyst for Hydrocracking of LDPE Plastic Waste into Liquid Fuels, *Mater. Chem. Phys.*, (2018).

[5] Zepeda H. M. P., "Novel Mesoporous Catalysts for Vacuum Residue Hydrocracking", (2013).

[6] Francis J., Guillon E., Bats N., Pichon C., Corma A., Simon L.J., Design of Improved Hydrocracking Catalysts by Increasing the Proximity Between Acid and Metallic Sites, *Appl. Catal. A Gen.*, **409-410**: 140–147, (2011).

[7] Stanislaus A., Marafi A., Rana M.S., Recent Advances in the Science and Technology of Ultra Low Sulfur Diesel (ULSD) Production, *Catal. Today*, **153(1–2)**: 1–68 (2010).

[8] Corma A., Martínez A., Martínez-Soria V., Catalytic Performance of the New Delaminated ITQ-2 Zeolite for Mild Hydrocracking and Aromatic Hydrogenation Processes, *J. Catal.*, **200(2)**: 259-269 (2001).

[9] Ward J. W., Hydrocracking Processes and Catalysts, *Fuel Process. Technol.*, **35(1)**: 55–85 (1993).

[10] van Dijk A., de Vries A.F., van Veen J.A.R., Stork W. H. J., Blauwhoff P. M. M., Evaluation of Hydrocracking Catalysts in Recycle Tests, *Catal. Today*, **11(1)**: 129–139 (1991).

[11] Alvarez A. Ancheyta J., Simulation and Analysis of Different Quenching Alternatives for an Industrial Vacuum Gasoil Hydrotreater, *Chem. Eng. Sci.*, **63(3)**: 662–673 (2008).

[12] Nishijima A., Sato T., Yoshimura Y., Shimada H., Matsubayashi N., Imamura M., Sugimoto Y., Kameoka T., Nishimura Y., Two Stage Upgrading of Middle and Heavy Distillates over Newly Prepared Catalysts, *Catal. Today*, **27(1)**: 129-135 (1996).

[13] Gosselink J. W., van de Paverd A., Stork W.H.J., Mild Hydrocracking: Optimization of Multiple Catalyst Systems fFor Increased Vacuum Gas Oil Conversion, *Catalysts in Petroleum Refining*, **53**: 385–397 (1989).

[14] Sadighi S., Ahmad A., Rashidzadeh M., 4-Lump Kinetic Model for Vacuum Gas Oil Hydrocracker Involving Hydrogen Consumption, *Korean J. Chem. Eng.*, **27(4)**: 1099–1108 (2010).

[15] Olorunyolemi T., Kydd R. A., The Effect of fluoride Addition on the Catalytic Activity of Gallium-Aluminium Mixed Oxides and Ni-Mo Supported on Them. *Catalysis Letters*, **63**: 173–178 (1999).

[16] Okamoto Y. and Imanaka T., Interaction Chemistry Between Molybdena and Alumina: Infrared Studies of Surface Hydroxyl Groups and Adsorbed Carbon Dioxide on Aluminas Modified with Molybdate, Sulfate, or Fluorine Anions, *J. Phys. Chem.*, **92(25)**: 7102–7112 (1988).

[17] Bookman P.M., Kydd R.A., Sarbak Z., Somogyvari A., Surface Acidity and Cumene Conversion: II. A Study of γ-Alumina Containing Fluoride, Cobalt, and Molybdenum Additives: the Effect of Reduction, *J. Catal.*, **100(2)**: 287–292 (1986).

[18] Lewis J. M., Kydd R. A., Boorman P. M., A Study of fluorided $NiMOAl_2O_3$ Catalysts in Cumene Conversion and Thiophene HDS Reactions, *J. Catal.*, **120(2)**: 413-420 (1989).

[19] Dik P.P., Klimov O.V., Koryakina G.I., Leonova K.A., Pereyma V.Yu., Budukva S.V., Gerasimov E.Yu., Noskov A.S., Composition of Stacked Bed for VGO Hydrocracking with Maximum Diesel Yield, *Catal. Today*, **220–222**: 124–132 (2014).

[20] Barkhordari A., Fatemi S., Daneshpayeh M., Zamani H., Development of a Kinetic Model for Modeling the Industrial VGO Hydrocracker Accompanied by Deactivation, *International Journal of Chemical Reactor Engineering*, **8**: (2010).

[21] Chen Y.-W., Tsai M.-C., Hydrotreating of Residue Oil over Aluminum Borate-Supported CoMo and NiMo catalysts, *Catal. Today*, **50(1)**: 57–61 (1999).

[22] Lewandowski M., Sarbak Z., Effect of Boron Addition on Hydrodesulfurization and Hydrodenitrogenation Activity of $NiMo/Al_2O_3$ Catalysts, *Fuel*, **79**: 487–495 (2000).

[23] Ferdous D., Dalai A.K., Adjaye J., A Series of $NiMo/Al_2O_3$ Catalysts Containing Boron and Phosphorus: Part I. Synthesis and Characterization, *Appl. Catal. A Gen.*, **260(2)**: 137–151 (2004).

[24] Ferdous D., Dalai A. K., Adjaye J., Comparison of Product Selectivity During Hydroprocessing of Bitumen Derived Gas Oil in the Presence of $NiMo/Al_2$ O_3 Catalyst Containing Boron and Phosphorus, *Fuel*, **85(9)**: 1286-1297 (2006).

[25] Palcheva R., Kaluža L., Spojakina A., Jirátová K., and Tyuliev G., $NiMo/\gamma\text{-}Al_2O_3$ Catalysts from Ni Heteropolyoxomolybdate and Effect of Alumina Modification by B, Co, or Ni, *Cuihua Xuebao/Chinese J. Catal.*, **33(6)**: 952-961 (2012).

[26] Chen W., Maugé F., Gestel J., Nie H., Li D., Long X., Effect of Modification of the Alumina Acidity on the Properties of Supported Mo and CoMo Sulfide Catalysts, *J. Catal.*, **304**: 47–62 (2013).

[27] Looi P.Y., Mohamed A.R., Tye C.T., Hydrocracking of Residual Oil Using Molybdenum Supported over Mesoporous Alumina as a Catalyst, *Chem. Eng. J.*, **181–182**: 717–724 (2012).

[28] Tailleur R. G., Hydrocracking Catalyst to Produce High Quality Diesel Fraction, *Scientific Bases for the Preparation of Heterogeneous Catalysts*, **143**: 321–329 (2002).

[29] Panariti N., Del Bianco A., Del Piero G., Marchionna M., Petroleum Residue Upgrading with Dispersed Catalysts: Part 1. Catalysts Activity and Selectivity, *Appl. Catal. A Gen.*, **204(2)**: 203–213 (2000).

[30] Koltunov K.Y., Sobolev V.I., Efficient Cleavage of Cumene Hydroperoxide over HUSY Zeolites: The Role of Brønsted Acidity, *Appl. Catal. A Gen.*, **336(1)**: 29–34 (2008).

[31] Weitkamp J., Ernst S., Factors Influencing the Selectivity of Hydrocracking in Zeolites, *MA: Springer US*, 343–354 (1990).

[32] Fatemi S., Abolhamd G., Moosavian M.A., Mortazavi Y., The Effect of Coking on Kinetics of HDS Reaction under Steady and Transient States, *Iran. J. Chem. Chem. Eng.*, **23**: 1–11 (2004).